

SIMCor

In-Silico testing and validation of Cardiovascular IMplantable devices

Call: H2020-SC1-DTH-2018-2020 (*Digital transformation in Health and Care*)

Topic: SC1-DTH-06-2020 (*Accelerating the uptake of computer simulations for testing medicines and medical devices*)

Grant agreement No: 101017578

Deliverable 6.4

Specification and quantification of subject-specific data-based boundary conditions

Due date of delivery: 31 December 2022

Actual submission date: 22 December 2022

Start of the project: 1 January 2021

End date: 31 December 2023



Reference

Name	SIMCor_D6.4_Specification-of-boundary-conditions_CHA_22-12-2022
Lead beneficiary	Charité – Universitätsmedizin Berlin (CHA)
Author(s)	Leonid Goubergrits (CHA), Jan Brüning (CHA)
Dissemination level	Public
Type	Report
Official delivery date	31 December 2022
Date of validation by the WP Leader	22 December 2022
Date of validation by the Coordinator	22 December 2022
Signature of the Coordinator	

Version log

Issue date	Version	Involved	Comments
25/11/2022	1.0	Jan Brüning (CHA), Leonid Goubergrits (CHA)	First draft by CHA
13/12/2022	2.0	Wouter Huberts (TUE)	Internal review
20/12/2022	3.0	Jan Brüning (CHA), Leonid Goubergrits (CHA)	Revised draft
21/12/2022	4.0	Anna Rizzo (LYN)	Formal review by LYN
22/12/2022	Final	Jan Brüning (CHA)	Submission by the PC

Executive summary

This document describes the assessment of boundary conditions required for in-silico assessment of device efficacy and safety for both project use cases, *transcatheter aortic valve implantation* (TAVI) and *pulmonary artery pressure sensor* (PAPS), using patient-specific information. These requirements include the patient- and subject-specific anatomy, i.e., the surface geometries of either the aorta or the pulmonary artery, as well as relevant functional boundary conditions, such as patient-specific volume flow rates in both the aorta and pulmonary artery, and pressure waveforms measured in the left ventricle and the aorta. The computational domains (i.e., anatomical geometries) and functional boundary conditions are used in the different models to assess the clinical endpoints selected for the two use-cases, as well as the validation of the respective models and virtual cohorts. All required information is either directly processed from medical image data and catheter-based pressure measurements or is calculated using hybrid approaches combining subject-specific measurements with models. All data is provided to all project partners via the *virtual research environment* (VRE). The VRE data allocation is also described in this document.

Table of contents

INTRODUCTION	5
TAVI USE CASE DATA	6
PATIENT-SPECIFIC ANATOMY.....	6
<i>Calcification map</i>	<i>7</i>
PATIENT-SPECIFIC BOUNDARY CONDITIONS - FLOW RATES.....	9
PATIENT-SPECIFIC BOUNDARY CONDITIONS - PRESSURE CURVES	9
PAPS HUMAN DATA.....	11
PATIENT-SPECIFIC ANATOMY.....	11
PATIENT-SPECIFIC BOUNDARY CONDITIONS - FLOW RATES.....	13
PAPS ANIMAL DATA.....	15
SUBJECT-SPECIFIC ANATOMY.....	15
<i>Retrospective cohort</i>	<i>15</i>
<i>Prospective animal cohort (chronic)</i>	<i>17</i>
SUBJECT-SPECIFIC FLOW RATES.....	18
<i>Retrospective cohort</i>	<i>18</i>
<i>Prospective animal cohort (chronic)</i>	<i>18</i>

List of figures

FIGURE 1: VISUALISATION OF THE DIFFERENT RECONSTRUCTION APPROACHES FOR THE TAVI USE CASE USED BY UCL (LEFT) AND CHA (RIGHT).....	7
FIGURE 2: EXEMPLARY VISUALISATIONS OF THE CALCIFICATION NODULES RECONSTRUCTED AT CHA (LEFT) AND UCL (RIGHT). THE ANATOMY OF THE LEFT VENTRICLE AND AORTA IS DEPICTED IN GREY, WHEREAS THE AORTIC VALVE LEAFLETS ARE DEPICTED IN BLUE AND THE CALCIFICATION NODULES IN BRIGHT RED.....	8
FIGURE 3: CALCULATION OF CALCIFICATION MAPS ON THE AORTIC VALVE LEAFLETS.....	8
FIGURE 4: COMPARISON OF A SIMPLIFIED ASCENDING AORTA WAVEFORM GENERATED USING A PARABOLIC FLOW ASSUMPTION AND THE STROKE VOLUME AND HEART RATE MEASUREMENTS. THE CONTINUOUS BLUE LINE INDICATES THE 4D FLOW MRI MEASUREMENT FOR THE PATIENT, WHEREAS THE DASHED LINES.....	9
FIGURE 5: ILLUSTRATION OF SIX EXEMPLARY, PATIENT-SPECIFIC PRESSURE WAVEFORMS MEASURED IN THE ASCENDING AORTA (BLUE) AND THE LEFT VENTRICLE (ORANGE).....	10
FIGURE 6: EXEMPLARY SURFACE MESH OF A HUMAN PA.....	11
FIGURE 7: EXEMPLARY GEOMETRY OF THE HUMAN PA AND ITS CORRESPONDING CENTRELINE AND A DEFINITION OF GEOMETRIC PARAMETERS CHARACTERISING THE PA GEOMETRY.....	12
FIGURE 8: DISTRIBUTION OF MAJOR GEOMETRIC PARAMETERS DESCRIBING THE SHAPE OF THE PA. BOX-PLOTS REPRESENTATION IS SELECTED FOR NORMALLY DISTRIBUTED PARAMETERS, WHEREAS HISTOGRAMS ARE USED FOR REPRESENTATION OF NOT-NORMALLY DISTRIBUTED PARAMETERS. LPA DIAMETERS, WHICH WERE NOT-NORMALLY DISTRIBUTED, WERE ALSO REPRESENTED AS THE BOXPLOT FOR THE COMPARISON WITH MPA AND RPA DIAMETERS.....	13
FIGURE 9: AVERAGE PULMONARY ARTERY WAVEFORM CALCULATED FROM 60 INDIVIDUAL MEASUREMENTS OBTAINED FROM HF PATIENTS.....	14
FIGURE 10: EXEMPLARY SURFACE MESH OF A PORCINE PA.....	15
FIGURE 11: DISTRIBUTION OF GEOMETRIC PARAMETERS DESCRIBING THE SHAPE OF THE PORCINE PA. BOX-PLOTS REPRESENTATION IS SELECTED FOR NORMALLY DISTRIBUTED PARAMETERS, WHEREAS HISTOGRAMS ARE USED FOR REPRESENTATION OF NOT-NORMALLY DISTRIBUTED PARAMETERS. MPA DIAMETERS, WHICH WERE NOT-NORMALLY DISTRIBUTED, WERE ALSO REPRESENTED AS THE BOXPLOT FOR THE COMPARISON WITH LPA AND RPA DIAMETERS.....	16
FIGURE 12: DISTRIBUTION OF MAJOR GEOMETRIC PARAMETERS DESCRIBING THE SHAPE OF THE PORCINE PA TREE IN THE PROSPECTIVE PRECLINICAL TRIAL WITH 10 PIGS.....	17
FIGURE 13: RECONSTRUCTED SURFACES OF ALL 10 PORCINE PA TREES FROM THE PROSPECTIVE ANIMAL STUDY.....	17
FIGURE 14: EXEMPLARY WAVEFORM MAPPED TO ONE SPECIFIC ANIMAL. THE AVERAGE WAVEFORM REFLECTS THE AVERAGE OF ALL 29 INDIVIDUAL FLOW RATES. THE RED LINES INDICATE THE STANDARD DEVIATION. PLEASE NOTE THAT THESE ARE NO VALID WAVEFORMS FOR THE SPECIFIC ANIMAL BUT RATHER INDICATE THE VARIATION FOR EACH GIVEN TIME-STEP, AS THE STROKE	

VOLUME WILL BE DIFFERENT COMPARED TO THE AVERAGE WAVEFORM. THE INDIVIDUAL WAVEFORMS ARE CHARACTERISED BY STEEPER SLOPES AND SHIFTED POSITIONS OF MAXIMUM FLOW RATES..... 18

List of tables

TABLE 1: CT-BASED PARAMETERS USED TO DEFINE PA INLET FLOW RATE..... 19

Acronyms

Acronym	Full name
AV	Aortic valve
CHA	Charité - Universitätsmedizin Berlin
CT	Computed tomography
CO	Cardiac output
HR	Heart rate
LV	Left ventricle
LPA	Left pulmonary artery
LVEDV	Left ventricle end-diastolic volume
LVESV	Left ventricle end-systolic volume
MPA	main pulmonary artery
MRI	Magnetic resonance imaging
PA	Pulmonary artery
PAPS	Pulmonary artery pressure sensor
PVL	Paravalvular leakage
RPA	Right pulmonary artery
SV	Stroke volume
TAVI	Transcatheter aortic valve implantation
TUE	Technische Universiteit Eindhoven
VRE	Virtual research environment

Introduction

Deliverable 6.4 continues the description of the data processing workflow of WP6 which aims to provide the necessary subject- and patient-specific data, as well as synthetic data sets, for the subsequent use in the in-silico models for virtual cohort generation (WP7), device implantation (WP8) and device effect simulation (WP9). The deliverable focuses on the processing of subject- and patient-specific computational domains and boundary conditions, which are derived from the retrospective patient data obtained at UCL and CHA, as well as retrospective and prospective animal data obtained at CHA. The required information for both the *transcatheter aortic valve implantation* (TAVI) and *pulmonary artery pressure sensor* (PAPS) use case includes anatomical models that were generated from *computed tomography* (CT) data, as well as hemodynamical information that is required to run the models, such as volume flow rates and invasively measured pressures. Hereby, the processing aims to populate the *D6.2 - Database for anatomy and function based on preclinical and clinical data* (CHA, M12), following the conventions specified in this document to ensure maximal interoperability of the data within the project as well as afterwards. Furthermore, the *D6.1 - Specification of data-processing requirements* (CHA, M4), as well as the considerations from *D6.3 -uncertainty quantification for input data* (CHA, M21), are applied throughout the processing. The specification of the boundary conditions required for future in-silico trials is separated into two sections, describing anatomical and functional data separately for each of two use cases.

TAVI use case data

Patient-specific information for the TAVI use case is available from both clinical centres UCL and CHA. However, the respective data sets vary both with respect to the available data elements as well as the performed processing procedures. These differences are described in detail in the two deliverables *D5.1 - Protocol for clinical data collection (CHA, M3)* and *D5.5 - Report on retrospective clinical data collection (CHA, M18)*. The main difference with respect to processing of boundary conditions is that pressure waveforms measured within the ascending aorta and the left ventricle are only available for a large subset of the patient records collected from CHA. General hemodynamic information, such as echocardiographic measurements of ventricular volumes, ejection fractions and heart rates, are available from both clinical centres. Furthermore, 4D flow MRI measurements of the volume flow rate across the aortic valve are not yet part of clinical routine. However, sufficient data sets of such measurements are available also for aortic stenosis patients, even though not for all patients.

For the different models, different anatomical, hemodynamic, and mechanical information are required to adequately describe the boundary conditions. For example, the exemplary virtual cohort generator for the TAVI use case, described in *D7.6 - Proof of principle of the complete virtual patient generator (TUE, M24)*, will require only clinical routine information as well as anatomical information from the CT-based reconstructions, as it uses a surrogate model for quantification of the outcome parameters such as the transvalvular pressure gradient. For the high-fidelity CFD models for assessing thrombosis, transient information on the blood flow across the valve is necessary to adequately model washout of the aortic sinuses, whereas exact information of the pressure gradient across the aortic valve during diastole might not be as relevant for adequately modelling valve closure. For modelling of the TAVI implantation procedure, information on patient-specific calcification patterns is important to model the structure-structure interaction between the device and the (calcified) tissue. Finally, pressure information in the left ventricle and aorta is vital for modelling the paravalvular leakage, as the resulting pressure gradient will directly affect the regurgitant volume.

Patient-specific anatomy

Reconstruction of the patient-specific anatomy followed two different approaches at the respective clinical centres. As both centres had access to more than 100 patient-specific data sets, data sets were not merged, so to have 2 dedicated data sets for the subsequent self-validation envisaged in Phase III of the project. Furthermore, as reconstruction procedures for the TAVI anatomies were already described in previous deliverables, such as *D5.6 - Completion of synthetic data creation process (UCL, M18)*, they will be only summarised here. While UCL performed mostly manual reconstruction of the ascending aorta, the aortic valve and the left ventricle, CHA used a parametric model for reconstruction of the aortic root, the aortic valve as well as the aorta (see *Figure 1*). While UCL provided thin-walled geometries reflecting the myocardium and vessel wall, CHA provided geometries of the blood-pool. Both approaches have their respective advantages and disadvantages considering specific in-silico models. For example, the blood-pool geometries can directly be used for CFD simulations of the intra-aortic hemodynamics, whereas the thin-walled geometry might be advantageous for finite element modelling of the tissue. However, both reconstruction approaches can be converted from one to the other, for example by extracting the inner boundary of the thin-walled geometries or extruding the surfaces of the blood-pool-only reconstructions.

All surface geometries are provided as STL files via the VRE. Dedicated folders for CHA and UCL were generated (Data@UCL, Data@CHA), which then contain a common folder structure containing all relevant information. The surface geometries are provided following the SIMCor naming convention in one respective subfolder for each clinical centre.

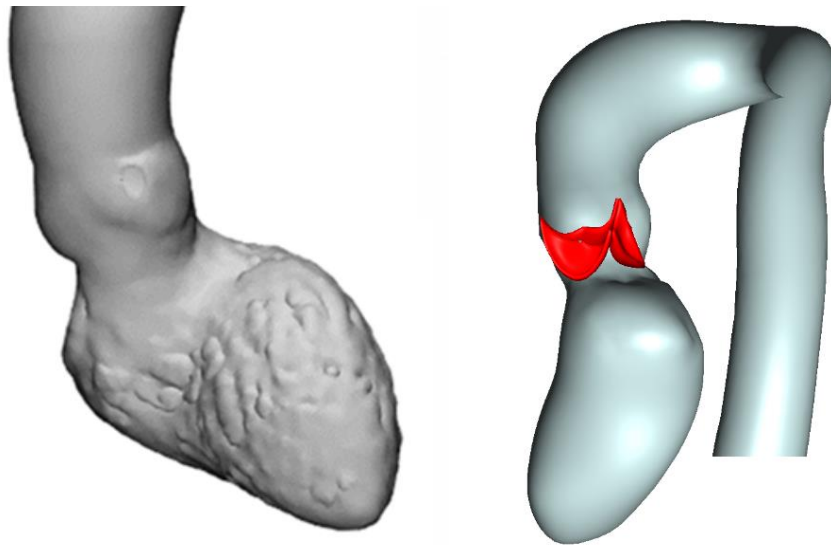


Figure 1: Visualisation of the different reconstruction approaches for the TAVI use case used by UCL (left) and CHA (right).

Several measurements of anatomical structures, such as the cross-sectional area of the aortic valve, diameters of the sinotubular junction and the left ventricular outflow tract are available from these reconstructions, CT image data as well as echocardiographic assessment. Assessment of these parameters was performed using varying approaches, ranging from clinical routine protocols for echocardiography, to manual and fully automated measurement of geometric parameters. Distributions of the most relevant of those parameters were already provided in *D5.5 - Report on retrospective clinical data collection (CHA, M18)*. Here, also a comparison of the two cohorts against each other and against relevant TAVI trial cohorts was provided. All individual data elements are provided within one Excel file per clinical centre (e.g., *[TAVI, CHA]_completeInformation.xlsx*). While these anatomical descriptors and measurements might not be a boundary condition in their own sense, they are vital for specifying the physiological envelope for the filtering approaches, and the validation steps, of the virtual cohort generators and are therefore also mentioned in this report.

Calcification map

Calcifications of the aortic root and aortic valve are of special interest for the in-silico modelling of device effect and safety. While the calcification will not directly affect the hemodynamics, they will alter the results of the device implantation simulation, as they are way stiffer than the tissue of the myocardium, the aorta, and the aortic valve. Calcifications were shown to be an independent predictor of *paravalvular leakage (PVL)*¹. As described in *D6.3 - Uncertainty quantification for input data (CHA, M21)*, reconstruction of calcifications from CT angiography is not entirely standardised, as no fixed threshold for reconstruction of the calcification nodules exists, but is relatively robust, nonetheless.

Calcification volumes

Clinically, mostly the calcification volumes are of interest, as this parameter was found to be directly correlated with the post-procedural PVL. Calcification volumes are specified for both data sets. This information is already of interest for some of the models to be developed and utilised in SIMCor, such as the IGA model for TAVI deployment. As this model uses coarse description of the aortic valve leaflets, the stiffness of the leaflets or parts of them can be modified according to the patient-specific calcification volume, making leaflets and annuli of patients with high calcification volumes stiffer than

¹Bhushan S, Bhushan S, Huang X, Li Y, He S, Mao L, Hong W, Xiao Z. Paravalvular Leak After Transcatheter Aortic Valve Implantation Its Incidence, Diagnosis, Clinical Implications, Prevention, Management, and Future Perspectives: A Review Article. *Curr Probl Cardiol.* 2022 Oct;47(10):100957. doi: 10.1016/j.cpcardiol.2021.100957.

the others. This information is provided in the same Excel tables as the general demographic, anatomic and hemodynamic patient-information.

Spatially resolved calcification information

In contrast to clinical assessment of the PVL risk, in-silico modelling allows to account for the patient-specific calcification location and sizes. In the models used for TAVI device implantation, which are described in *D8.6 - Report on 3D finite element simulation (PHI, M24)*, 3D reconstructions of the calcification nodules are required to adequately model the device and vessel deformation due to the implantation procedure. These calcification nodules were reconstructed from CT images like the other anatomical structures, as they are characterised by very high contrasts. Separate STL files for the calcification can be generated and are provided together with the surface geometries without calcifications (see *Figure 2*). This approach allows assessment of the effect of the calcification on the implantation procedures independently of the overall anatomy.

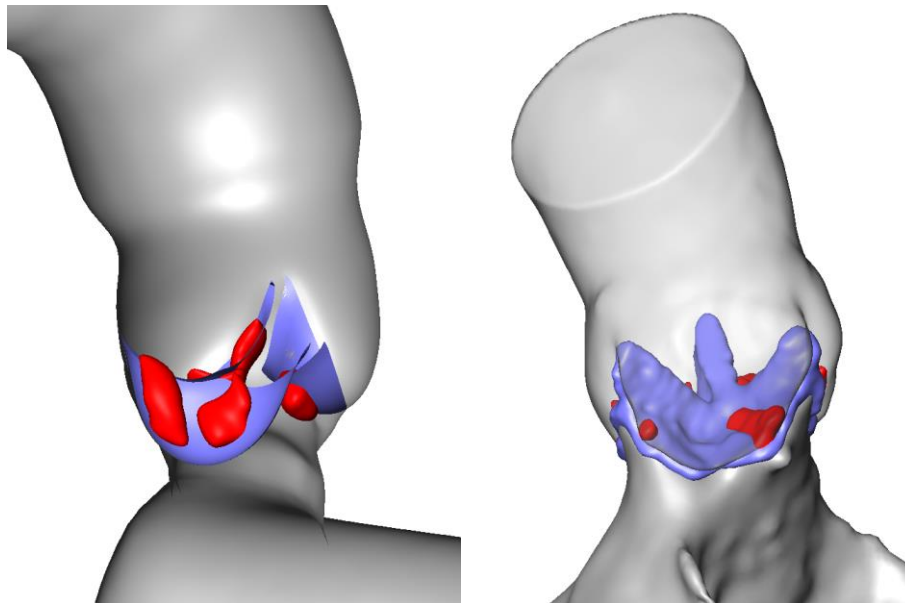


Figure 2: Exemplary visualisations of the calcification nodules reconstructed at CHA (left) and UCL (right). The anatomy of the left ventricle and aorta is depicted in grey, whereas the aortic valve leaflets are depicted in blue and the calcification nodules in bright red.

From these calcification nodules, also calcifications maps can be calculated, which allow to assess which part of the aortic root or aortic valve leaflets are affected by calcifications (see *Figure 3*). While this approach is not yet used in the consortium for the device implantation simulations, it is currently evaluated as one approach for generation of synthetic calcification nodules, by learning and subsequent mapping of the stochastic calcification distributions. And is therefore briefly mentioned.

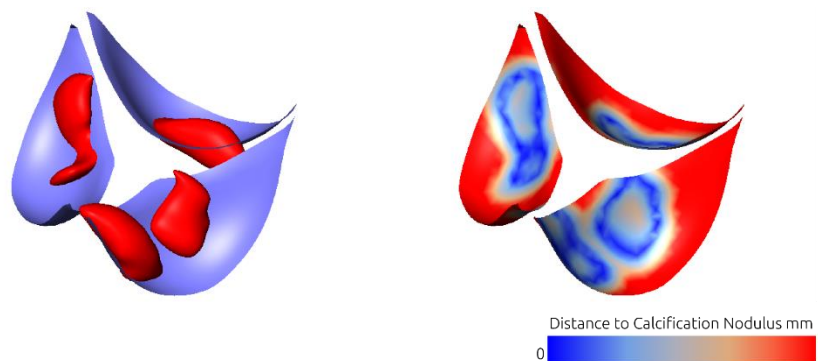


Figure 3: Calculation of calcification maps on the aortic valve leaflets.

Patient-specific boundary conditions - flow rates

While no 4D flow MRI information is available for all TAVI patients, echocardiographic measurements of the key hemodynamic parameters describing the aortic flow are available from clinical routine. These include measurements of the stroke volume and the heart rate. From these measurements transient volume flow information can be calculated using different approaches. First, the systolic phase of the aortic volume flow is characterised by a parabolic profile, with a faster acceleration than deceleration phase. The duration of the acceleration phase is approximately one third of the systolic ejection period. Assuming that no significant aortic regurgitation occurs, an artificial waveform can be generated for all patients based on the heart rate as well as the stroke volume. An exemplary waveform is shown in *Figure 4*.

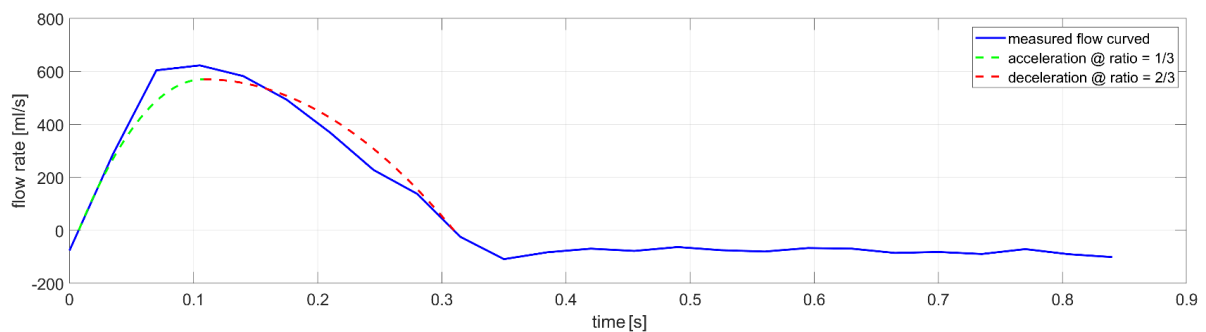


Figure 4: Comparison of a simplified ascending aorta waveform generated using a parabolic flow assumption and the stroke volume and heart rate measurements. The continuous blue line indicates the 4D flow MRI measurement for the patient, whereas the dashed lines.

While this approach will result in deviations in the exact flow waveform, these deviations are considered to be neglectable for two reasons. First, while 4D flow MRI provides transient information on the patient-specific volume flow rate in the ascending aorta, this measurement technique is associated with a low measurement accuracy and errors of 10% and higher are possible even in well-controlled in-vitro setups². Furthermore, measurements during MRI are usually performed at absolute rest. However, the intra-patient variation of the flow rate and ejection mechanics is large and can be affected by diet, blood pressure as well as the heart rate (e.g., exercise). As the aim is to model thrombosis after TAVI implantation, which is a process that occurs at time scales multiple orders of magnitudes larger than one heartbeat, modelling ‘the exact’ waveform is neither necessary nor possible. Providing a physiological envelope of the patient-specific flow waveforms is considered sufficient for the thrombosis modelling. Volume flow waveforms are made available via CSV files for each patient-specific anatomy via the VRE for both UCL and CHA use cases.

Patient-specific boundary conditions - pressure curves

Pressure information in the left ventricle and the ascending aorta are required for modelling of PVL, as the pressure gradient from ascending aorta to the left ventricle during diastole is directly correlated with the flow across the regurgitant orifices between the TAVI device and the aortic annulus. This information was obtained from invasive catheter measurements during the TAVI procedure. All measurements were performed before implantation of TAVI. Pressure waveforms were digitised from analogue printouts (exemplary pressure waveforms are shown in *Figure 5*). Overall, for 71 patients for which time-resolved CT data was available for reconstruction of the patient-specific anatomy, pressure measurements were also available. These measurements were taken before TAVI intervention, meaning that the systolic pressure gradient across the aortic valve is very high, which

² David A, Le Touze D, Warin-Fresse K, Paul-Gilloteaux P, Bonnefoy F, Idier J, Moussaoui S, Guerin P, Serfaty JM. In-vitro validation of 4D flow MRI measurements with an experimental pulsatile flow model. *Diagn Interv Imaging*. 2019 Jan;100(1):17-23.

becomes apparent by the larger pressures observed in the left ventricle rather than the ascending aorta. While the aim of the in-silico modelling is to assess the situation after the TAVI procedure, the data obtained pre-interventionally is still entirely sufficient, as the PVL is only occurring during diastole, where the left ventricular pressure is close to zero independent of the aortic stenosis and the ascending aorta pressure is generally not affected by the aortic stenosis. This pressure information is provided as CSV-file format (comma-separated values), containing the time, as well as the pressure information individually for left ventricle and the ascending aorta. At least two consecutive heart cycles were digitised per patient. If variation in heart cycles, either with respect to the R-R-intervals, i.e., the duration of the individual heart beats, or the pressure maxima, was observed, more cycles were digitised.

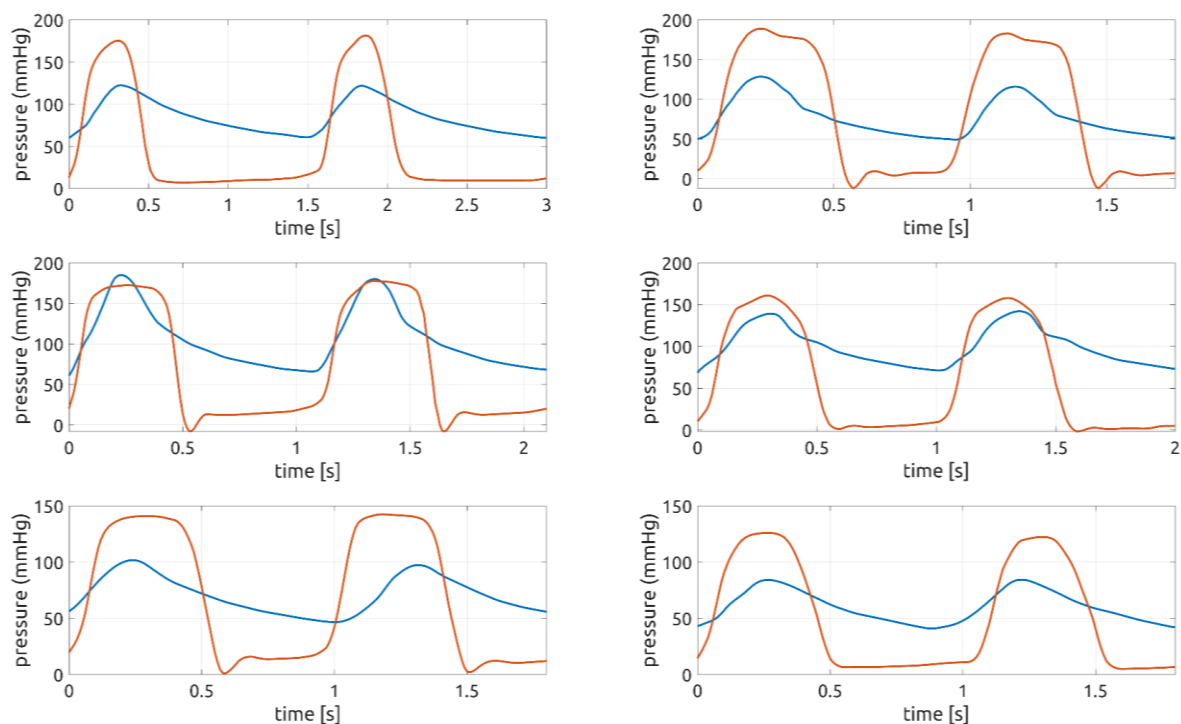


Figure 5: Illustration of six exemplary, patient-specific pressure waveforms measured in the ascending aorta (blue) and the left ventricle (orange).

PAPS human data

Retrospective data of 48 patients (age: 81 ± 7.6 years; sex: 20 female; weight: $76.2 + 18.0$ kg) that were acquired between February 2019 and October 2020 at CHA were used as basis for the in-silico modelling of the PAPS use case.

Patient-specific anatomy

Surfaces geometries of 48 PA, including main, left and right PA segments, as well as side branches of the second order, were reconstructed from CT image data. These surface geometries describe the boundary between the blood lumen and the vessel wall and are the major boundary condition for all in-silico modelling approaches of the PAPS use case, including sensor implantation simulation as well as simulation of the haemodynamic for assessment of thrombogenicity. All geometries are provided to the SIMCor consortium via the VRE³ using the STL file format. These files describe the surfaces as a triangulated mesh (*Figure 6*) with a spatial resolution, defined by the edge length of the triangles, of approximately 0.8 mm. Thus, the resulting mesh consists of approximately 60.000 triangles and 30.000 nodes. These meshes can be further modified according to the specific requirements of the respective model used in either WP8 or WP9.

In order to quantify the shape variance of the human cohort, a set of geometric parameters were calculated based on automatically generated PA centrelines (*Figure 7*). Definitions of geometric parameters selected to quantify PA geometry as well as a detailed description of the measurement procedure can be found in the deliverable D6.3.

Figure 8 shows distributions of the major geometric parameters of the human cohort, whereas a table ([PAPS]centerlinesInfo_human.xlsx) in the respective folder of the VRE contains all geometric parameters for each of 48 cases.

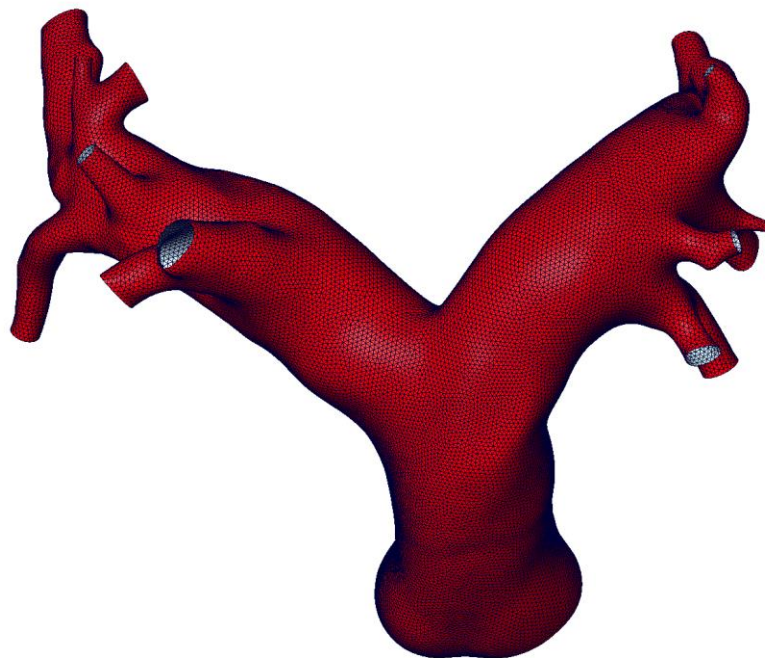


Figure 6: Exemplary surface mesh of a human PA.

³ data@CHA/[PAPS]pulmonaryArtery_human_real]/surfaceGeometry

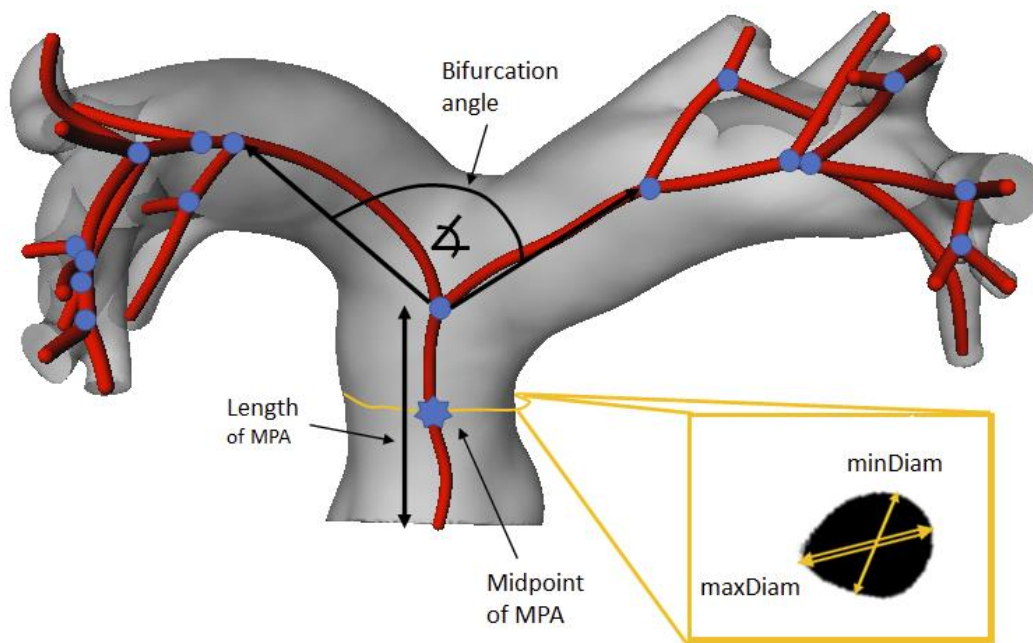


Figure 7: Exemplary geometry of the human PA and its corresponding centreline and a definition of geometric parameters characterising the PA geometry.

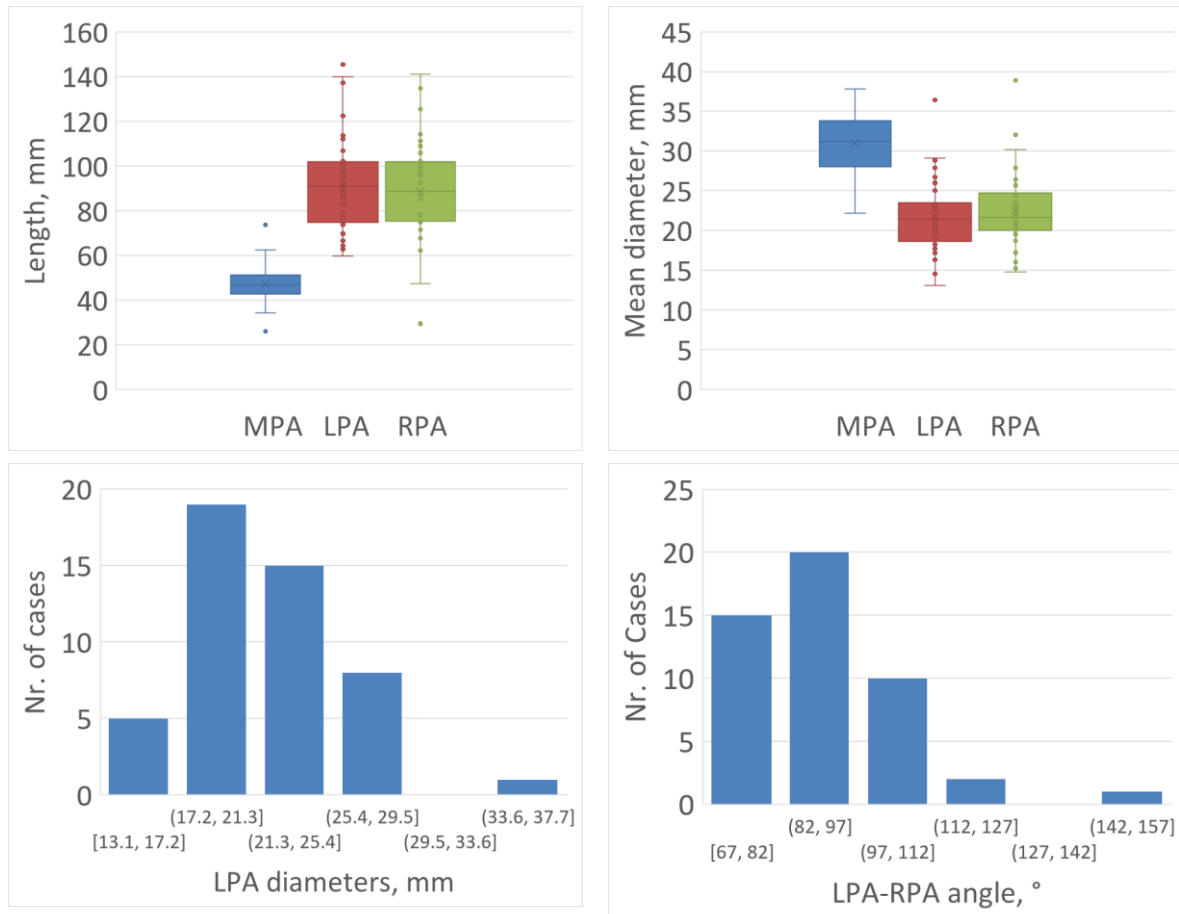


Figure 8: Distribution of major geometric parameters describing the shape of the PA. Box-plots representation is selected for normally distributed parameters, whereas histograms are used for representation of not-normally distributed parameters. LPA diameters, which were not-normally distributed, were also represented as the boxplot for the comparison with MPA and RPA diameters.

Patient-specific boundary conditions - flow rates

The approach for generation of transient volume flow information for the PAPS use case was similar to that for the TAVI use case. While volume flow rate measurements within the PA of 60 HF patients were available, no CT measurements were available for this patient data set. However, the pulmonary artery could only be reconstructed from CT data sets with sufficient quality, meaning that transient volume flow information had to be mapped from clinical routine measurements of the patient-specific haemodynamics, such as HR and SV. For this, an average waveform of the PA volume flow rate (see Figure 9) was generated and subsequently used as a template. The waveform was then scaled to match the patient-specific cardiovascular measurements of stroke volume and heart rate. These individual waveforms are made available via the VRE.

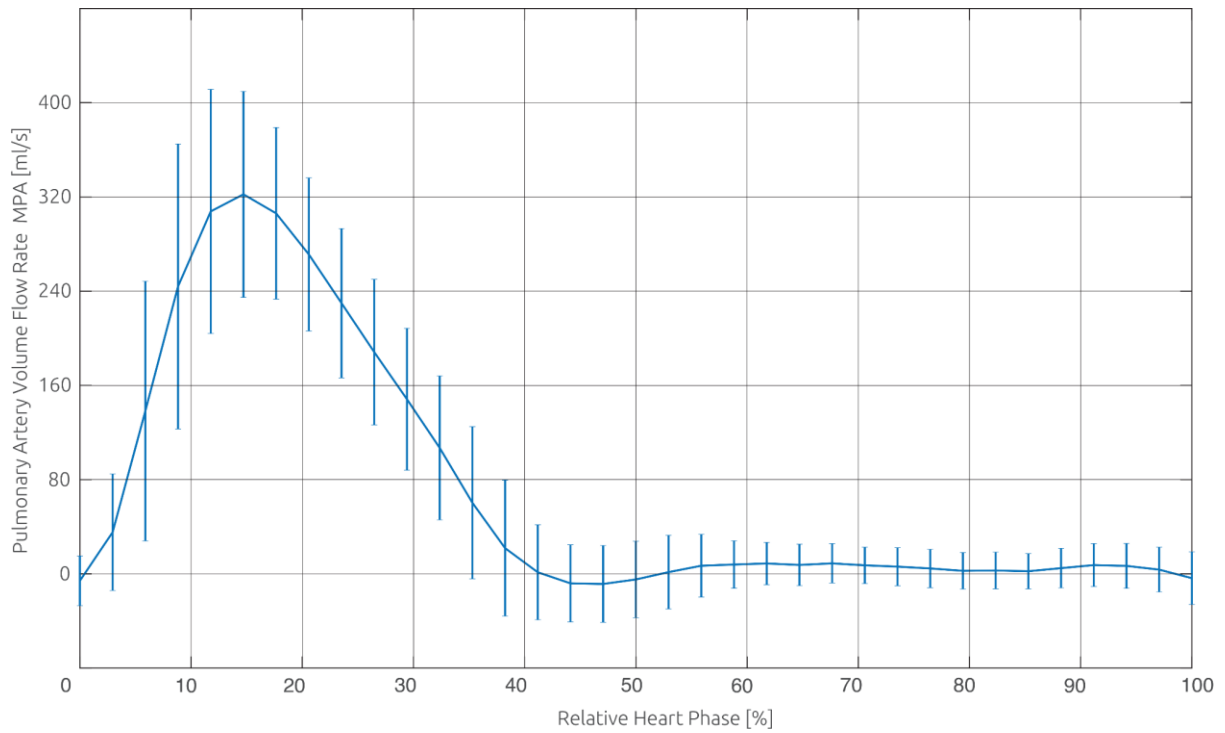


Figure 9: Average pulmonary artery waveform calculated from 60 individual measurements obtained from HF patients.

PAPS animal data

A porcine animal model was proposed for the pre-clinical testing of the PAPS. Three different cohorts of porcine data were available in SIMCor:

1. A retrospective cohort of CT data of 41 domestic pigs (82.6 ± 18.8 kg) with systolic and diastolic phases used for the analysis of the shape variance.
2. A retrospective cohort of 4D flow MRI data of 29 pigs (39.8 ± 15.5 kg) with flow curves measured at the main PA.
3. A cohort of CT data of 10 domestic pigs (62.1 ± 5.4 kg at the time of the PAPS implantation) with and without implanted PAPS acquired during the project. The measured weight of pigs during explantation (M3) was 125.2 ± 16.0 kg, whereas the interpolated weight of pigs during CT imaging at M1 after implantation was 83.1 ± 7.0 kg.

Subject-specific anatomy

Retrospective cohort

Surfaces geometries of 48 PA, including main, left and right PA segments, as well as side branches of the second order, were reconstructed from CT image data. These surface geometries describe the boundary between the blood lumen and the vessel wall and are the major boundary condition for all in-silico modelling approaches of the PAPS use case, including sensor implantation simulation as well as simulation of the hemodynamics for assessment of thrombogenicity. Furthermore, these geometries were used to generate a statistical shape model of the porcine PA allowing generation of synthetic PA geometries. All geometries are provided to the SIMCor consortium via the VRE⁴ using the STL file format. These files describe the surfaces as a triangulated mesh (*Figure 10*) with a spatial resolution that was equal to that of the human PA anatomies.

In order to quantify the shape variance of the retrospective porcine cohort, the same geometric parameters of the human cohort were calculated based on the automatically generated PA centrelines.

Figure 11 shows distributions of the geometric parameters of the retrospective porcine cohort, whereas an Excel file [PAPS]centerlinesInfo_porcine.xlsx in the respective folder of the VRE contains all geometric parameters for each of the 41 cases.

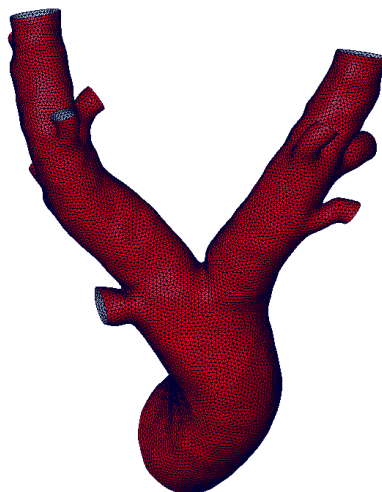


Figure 10: Exemplary surface mesh of a porcine PA.

⁴ data@CHA/[PAPS]pulmonaryArtery_porcine_real/retrospectiveCohort/surfaceGeometry

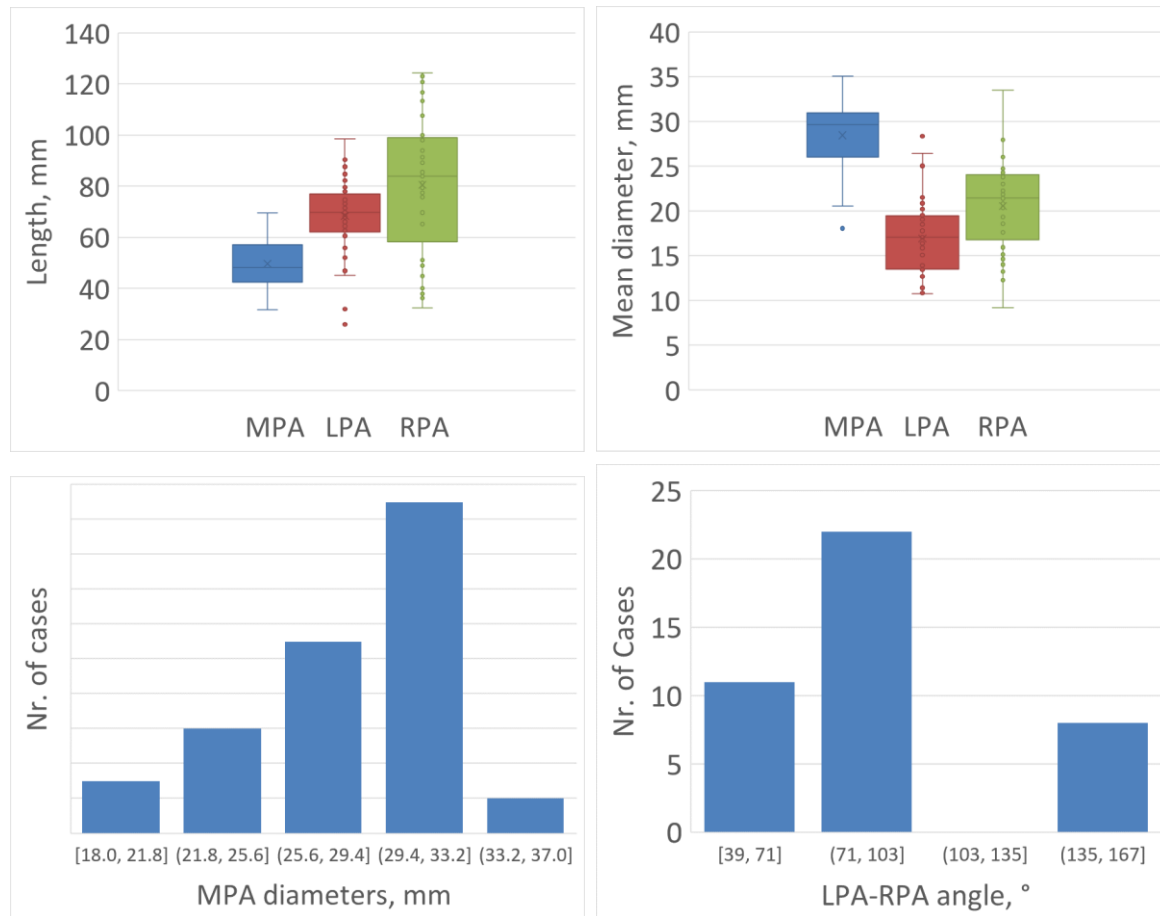


Figure 11: Distribution of geometric parameters describing the shape of the porcine PA. Box-plots representation is selected for normally distributed parameters, whereas histograms are used for representation of not-normally distributed parameters. MPA diameters, which were not-normally distributed, were also represented as the boxplot for the comparison with LPA and RPA diameters.

Prospective animal cohort (chronic)

Surfaces geometries of 10 porcine PA, including main, left, and right PA segments, as well as side branches of the second order, were reconstructed from CT image data (see *Figure 12*). These surface geometries describe the boundary between the blood lumen and the vessel wall and are the major boundary condition for all in-silico modelling approaches of the PAPS use case, including sensor implantation simulation as well as simulation of the haemodynamics for assessment of thrombogenicity. Furthermore, these geometries were used to generate a statistical shape model of the porcine PA allowing generation of synthetic PA geometries. All geometries are provided to the SIMCor consortium via the VRE⁵ using the STL file format.

Figure 13 shows distributions of these geometric parameters of the prospective porcine cohort, whereas an Excel file [PAPS]centerlinesInfo_porcine_prospective.xlsx in the respective folder of the VRE provides all individual geometric parameters for each of 10 cases.

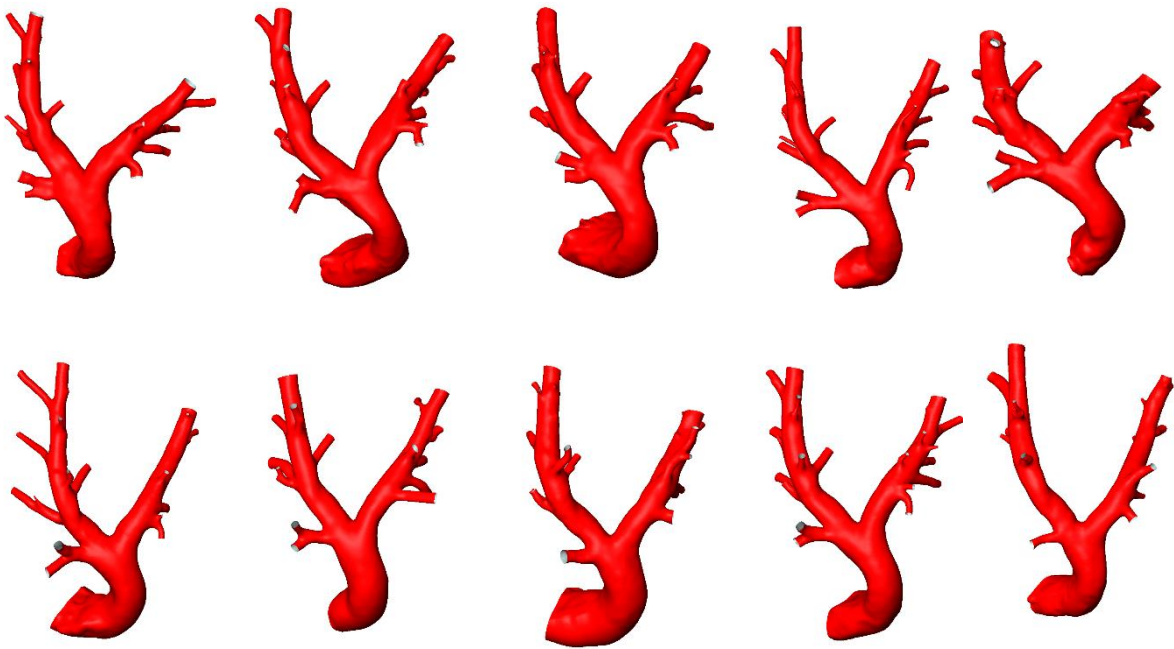


Figure 13: Reconstructed surfaces of all 10 porcine PA trees from the prospective animal study.

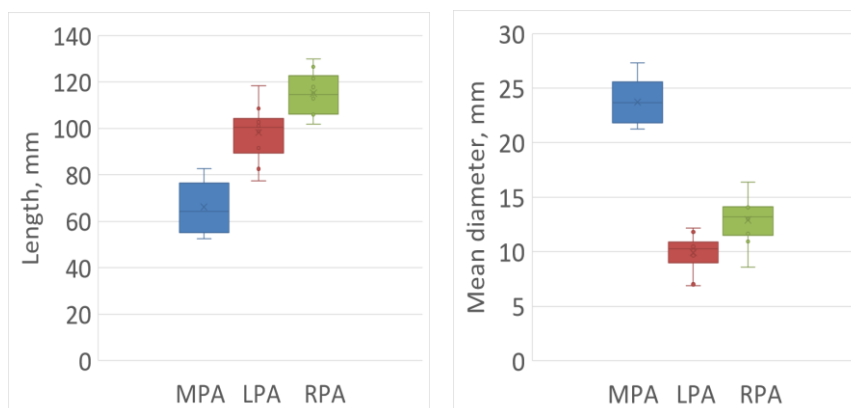


Figure 12: Distribution of major geometric parameters describing the shape of the porcine PA tree in the prospective preclinical trial with 10 pigs.

⁵ data@CHA/[PAPS]pulmonaryArtery_porcine_real]/prospectiveCohort/surfaceGeometry

Subject-specific flow rates

While several subject-specific flow waveforms measured using MRI were available from different retrospective, preclinical trials using porcine animal models, direct measurements of the flow rate were neither available for the retrospective data sets for which also well resolved CT information was available, nor for the prospective data sets. Due to the long imaging durations for 4D velocity encoded MRI as well as the difficulties of maintaining anaesthesia in the MRI (metallic/electric equipment might not be usable close to the scanner), no MRI measurements were considered for the chronic experiments and only two measurements will be performed for the acute experiments. Thus, the information of the subject-specific volume flow waveforms had to be adapted to the hemodynamic function of the respective animals by adapting the subject-specific waveforms from the MRI cohort to the subject-specific values for stroke volume, measured by reconstruction of the ventricular volumes, and heart rate, measured during the CT via ECG, and therefore adjusting the cardiac output (see *Figure 14*).

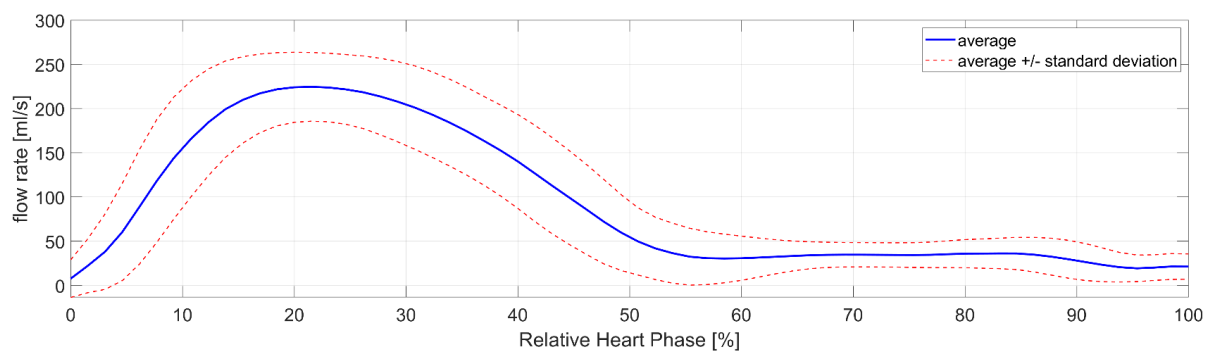


Figure 14: Exemplary waveform mapped to one specific animal. The average waveform reflects the average of all 29 individual flow rates. The red lines indicate the standard deviation. Please note that these are no valid waveforms for the specific animal but rather indicate the variation for each given time-step, as the stroke volume will be different compared to the average waveform. The individual waveforms are characterised by steeper slopes and shifted positions of maximum flow rates.

Retrospective cohort

For the retrospective animal porcine data sets, hemodynamic information of interest could not be estimated directly from the CT image data. Thus, SV and HR, and therefore the CO, were modelled according to their respective body weight⁶. While this approach is most likely associated with relative uncertainty, the retrospective data sets are solely used for generation of synthetic data sets. Here, the main interest is to have a data set that is covering the physiological envelope of the anatomy of the animals as well as the hemodynamic boundary conditions. The average as well as individual volume flow waveforms were scaled to the subject-specific estimates of the SV and HR and were made available via the VRE (data@CHA\[PAPS]pulmonaryArtery_porcline_real\retrospectiveCohort).

Prospective animal cohort (chronic)

A similar approach as for the retrospective cohort was used for the prospective cohort. However, as transient CT image data was available, the subject-specific HR as well as the stroke volume could be easily discerned. While the heart rate is directly measured, the stroke volume was measured by reconstruction of the left ventricular end-diastolic (LVEDV) and end-systolic volumes (LVESV). The difference of both values equals the stroke volume. As all animals were healthy with respect to the valvular function and no relevant regurgitant flows were to be expected, the left and right ventricular stroke volumes must be equal. Thus, neither SV nor HR had to be estimated from the animals' weight. Using this information, volume flow waveforms were calculated for all chronic animals and were uploaded to the VRE (data@CHA\[PAPS]pulmonaryArtery_porcline_real\prospectiveCohort). The

⁶ van Essen GJ, Te Lintel Hekkert M, Sorop O, Heinonen I, van der Velden J, Merkus D, Duncker DJ. Cardiovascular Function of Modern Pigs Does not Comply with Allometric Scaling Laws. *Sci Rep.* 2018 Jan 15;8(1):792. doi: 10.1038/s41598-017-18775-z

measurements used for calculation of the volume flow waveforms are specified in *Table 1* and are also uploaded to the VRE.

ID	LVEDV, ml	LVESV, ml	SV, ml	min HR, bpm	max HR, bpm	mean CO, L/min
CC1	97.2	27.0	70.2	122	127	8.74
CC2	105.0	24.0	81.0	93	97	7.69
CC3	94.5	29.3	65.2	109	111	7.17
CC4	108.0	40.7	67.3	104	108	7.13
C5	104.9	39.3	65.6	87	89	5.77
C6	86.5	29.6	66.9	107	109	7.23
C7	86.6	22.9	63.7	107	109	6.88
C8	100.7	37.4	63.3	100	103	6.42
C9	83.0	33.0	50.0	111	126	5.92
C10	113.3	50.6	62.7	109	112	6.93

Table 1: CT-based parameters used to define PA inlet flow rate.